DETERMINATION OF THE OPTICAL PROPERTIES OF MUSCLE PHANTOM BY KUBELKA-MUNK FUNCTION APPROACH

HÜSEYIN OKAN DURMUŞ[1,2,a)], BAKI KARABÖCE[2] & MIRHASAN Yu. SEYIDOV[1]
[1]Department of Physics, Gebze Technical University, 41400, Kocaeli, Turkey
[2]Medical Metrology Laboratory, TUBITAK National Metrology Institute (TUBITAK UME), 41470, Kocaeli, Turkey
E-mail: hokandurmus@gtu.edu.tr, smirhasan@gtu.edu.tr;
Tel : (262) 605 10 00; Fax: (262) 653 84 90

Tissue-mimicking materials, also known as phantoms, are widely utilized for device development, testing, performance assessment, calibration, and training, particularly in the medical industry. Phantoms are utilized as reference test materials in these investigations. Phantoms must be designed for whatever function they are intended to serve. For example, if they are to be used in the ultrasound field, they must have acoustical characterization, if they are to be used in the optical field, they must have optical characterization, and if they are to be used in the microwave field, they must have characterization of their dielectric properties. They must also be produced in line with the required characteristics of the tissues and organs for which they will be utilized and assessed as true phantoms. Three fundamental metrics, absorption coefficient, reduced scattering coefficient, and anisotropy factor, are regarded differentiating properties in optical characterization and are referred to as microscopic optical qualities in the literature. The macroscopic optical properties of the muscle phantom, such as absorbance, transmittance, reflectance, refractive index, and attenuation coefficient, were investigated using a spectrometer with a broadband white light source and a single integrating sphere in the wavelength range of 200 nm to 1000 nm. Then, using the Kubelka-Munk Function method, microscopic optical features such as absorption coefficient, scattering coefficient, and reduced scattering coefficient were estimated in the wavelength range of 200 nm to 1000 nm based on the data of these macroscopic characteristics. In this study, the findings of the macroscopic and microscopic optical properties of a muscle phantom, which are also compatible with the literature data, will be presented.

Keywords: Muscle Phantom, Microscopic and Macroscopic Optical Properties, Optical Characterization, Spectrometer, Single Integrating Sphere, Broadband White Light Source.

INTRODUCTION

Today, due to its non-invasive nature, optical technologies have started to be used more in the field of diagnosis, treatment and surgery in the medical field. Examples of these are clinical functional optical imaging such as spectroscopy and optical coherence tomography, laser surgery and phototherapy devices. For example, visualization of blood vessels and microcirculation, monitoring of blood oxygenation and tissue metabolism, imaging of skin cancer, drug tracking, and micro-vessel and particle distribution in diagnostic; photodynamic therapy (PDT), low level laser therapy (LLLT) and photothermal therapy (PTT) in therapy; In surgery, tissue laser ablation, coagulation and cutting can be given. However, the effective use of these devices in human tissues depends on a good study of tissue-light interactions. In other words, there is a great need for reliable data on the optical properties of human tissues and the prediction of light-absorbed energy distributions. For this reason, many new methods and techniques are being developed and investigated in the field of biomedical optics for the investigation of the optical properties of human tissues [1].

In the literature, there are many publications on the determination of optical properties of human and animal tissues such as skin and muscle [2], liver [3], lung [4], kidney [5], heart [6], brain [7], breast [8], blood vessel [9], prostate [10], bowel[11], bladder [12], bone [13] and tumor tissue [14].

Biological tissues are basically turbid in terms of optical transparency. Therefore, it is not easy to measure the optical properties of this complex turbid medium. These turbid environments are defined through fundamental optical properties such as scattering and absorption components, and these properties of biological tissues constitute an important research tool in biomedical diagnosis and therapy. So, accurate measurements of the optical properties of the turbid medium are important and typically, the light distribution in a diffuse medium can be modelled based on its intrinsic optical properties, including absorption coefficient ($\mu\alpha$), scattering coefficient (μs), anisotropy factor (g) and reduced scattering coefficient ($\mu s'$) [15-17].

There are generally two types of experimental techniques, direct and indirect, to measure the optical properties of tissues. Direct methods do not require any supporting models for the radiative transfer process and rely solely on experimental results. Whereas, indirect (inverse) methods always use a theoretical light scattering model used with experiment.The basic description underlying these experimental methods requires either measuring the emitted reflection from an irradiated turbid sample or transmittance through it [16]. Thus, to summarize, tissues are characterized in vitro using techniques such as the solution of the radiative transfer equation, integrating sphere spectroscopy, Kubelka-Munk (KM) model, the inverse adding-doubling (IAD) method and the inverse Monte Carlo (IMC) simulation [1, 17- 22].

131, H.Javid ave, AZ-1143, Baku
Institute of Physics
E-mail: jophphysics@gmail.com

Tissue-mimicking materials (TMMs) or tissue phantoms are widely used in the biomedical research area especially at thermo-acoustical [23-26] and optical research [27-30] as a test model.

The definition of the phantom is made as “any apparatus or material that mimics the operation or physical properties of human systems or tissues”. Although it is possible to use real tissues directly in experiments, this is not a logical method. Instead, working with artificial materials that simulate the physical properties (such as acoustical, optical, mechanical and thermal, etc.) of human tissues provides many benefits. Therefore, phantoms enable systematic testing and controlled optimization of new measurement methodologies before being tested on living things such as animals or humans. The use of phantoms enables simulation for systems at different complexity levels or human tissues. The use of phantoms in initial tests instead of biological materials provides an effective alternative to medical research. Therefore, after the initial results on phantoms are positive, real tissues can be used. After this stage, animal experiments (laboratory mice in general) are usually performed, and then the tests are performed on humans [31].

In the optical field, phantoms are used in various forms such as the development of imaging techniques and image-guided interventions, system validation, optimization, stability assessment, medical device calibration, verification, and clinical training [32-34].

Muscles in the human body have a unique structure and serve a specific purpose. There are around 600 muscles in the human body, accounting for about 40% of the total weight. Thousands or tens of thousands of tiny muscle fibers make up each muscle. A nerve controls each muscle fiber and permits the muscle to contract. In the human body, there are three types of muscles. These are heart muscle, smooth muscle, and skeletal muscle. Only skeletal muscles are voluntary, meaning they can be controlled consciously. Smooth and cardiac muscles are uncontrollably active. Skeletal muscle is a type of muscle that moves bones and other tissues. Skeletal muscles contract and relax, cling to the bones, and react to voluntary nervous system instructions. Internal organs can function thanks to smooth muscle tissue, which is found in organs like the stomach and bladder. The heart muscle contracts to pump blood around the body. Moving, standing, talking, breathing, chewing and digesting food, pumping blood in the heart, perceiving an item, and regulating our body temperature all require the muscular system. As a result, the muscular system is a sophisticated muscle network that is essential to the human body's survival. Eleven major functions are performed by the muscular system. Mobility, Stability, Posture, Circulation, Respiration, Digestion, Urination, Birth, Vision, Organ Protection, and Temperature Adjustment are among the functions stated [35-36].

The Kubelka-Munk model is a widely used theoretical reflectance model in optics. It is assumed in this model that some light traveling through a homogeneous sample is dispersed and absorbed in two directions, weakening the light. A two-flux approach to universal radiation transfer theory is the Kubelka-Munk model. The K - M scattering and absorption coefficients, which are denoted as S and K, respectively, describe the propagation of up and down fluxes. Radiation transfer models have been widely used to define the optical characteristics of light-scattering materials. The Kubelka and Munk model is one of the most successful and straightforward models. The optical characteristics of particulate films under diffused light may be calculated using this model, which uses the material's effective absorption and scattering coefficients. The Kubelka–Munk model has a wide range of applications in materials analysis, including paints, pigmented plastics or polymers, decorative and protective coatings, solar-absorbing pigments and paints, human tissue, leaves, biological systems, crystalline materials, solids, powders, fibrers and wool, papers, thermal insulation, and optical properties. The optical characteristics of the coating are considered to be represented by two constants in this model, the absorption and scattering coefficients [37-40]. The absorption coefficient (μa), scattering coefficient (μs), and scattering anisotropy factor (g) of tissue are the major variables influencing light propagation in the tissue. The degree of these characteristics is influenced by both tissue structure (scattering) and chromophore content (absorption) [41]. Three fundamental parameters are regarded differentiating features in optical characterization: absorption coefficient, reduced scattering coefficient, and anisotropy factor, and these parameters are referred to as microscopic optical properties in the literature [42].

In this study, macroscopic optical properties of muscle phantom such as absorbance, transmittance, reflection, refractive index and attenuation coefficient were investigated using a spectrometer with a single integrated sphere and a broadband white light source in the wavelength range of 200 nm to 1000 nm. Then, using the Kubelka-Munk Function method, microscopic optical properties such as absorption coefficient, scattering coefficient and reduced scattering coefficient were determined based on the data of these macroscopic properties. The fact that the microscopic optical properties determined based on very complex processes are relatively easier to detect using the Kubelka-Munk Function method is an important feature that distinguishes the study from its counterparts.

METHODOLOGY

In this study, the muscle phantom, a compact spectrometer, a broadband stabilized fiber-coupled white light source, a single integrating sphere and Thorlabs OSA software for optical evaluation were used. All experiments were performed under controlled laboratory ambient conditions.

PREPARATION OF MUSCLE PHANTOM

Tissue-Mimicking Material (TMM) is commonly employed as a test object in biomedical research

because of its capacity to imitate biological soft tissues. In this study, we used a muscle phantom identical to the one published by Gutierrez et al. [43]. The phantom's muscle-mimicking features were also validated acoustically. The sound speed was measured as 1550.9 48.4 m/s (Ref: 1547 m/s [44]). The phantom was prepared as follows. In a container, 2.3 g of agar and 10.7 g of aluminum oxide are combined with 125 mL of distilled water. With the aid of fish, the magnetic stirrer is progressively raised to 400 revolutions per minute. The temperature of the solution is raised until it reaches 80 degrees Celsius. When it hits 80 °C, the heat is turned off, and the temperature of the solution is anticipated to drop to 60 °C. A syringe is used to add 10 mL of glycerin to the solution at 60 °C. In the meantime, the solution is still being combined with the fish. When the solution reaches 40 degrees Celsius, it is poured into the phantom mold and let to freeze. Thickness of the muscle phantom specimen cut out as a sample was 20 mm.

THE OPTICAL CHARACTERIZATION SETUP

Optical equipment included a compact spectrometer (Thorlabs, CCS200/M) with a wavelength range of 200 nm to 1000 nm, a broadband stabilized fiber-coupled white light source (Thorlabs, SLS201L/M), and a single integrating sphere (Thorlabs IS200 type 2” integrating sphere). Figure 1 shows the experiment set-up, and Figure 2 shows how all the optical measurements and computations were realized using Thorlabs OSA software and MS Excel.

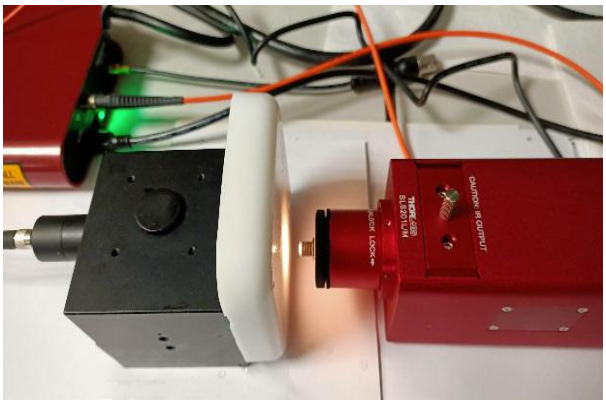

a)

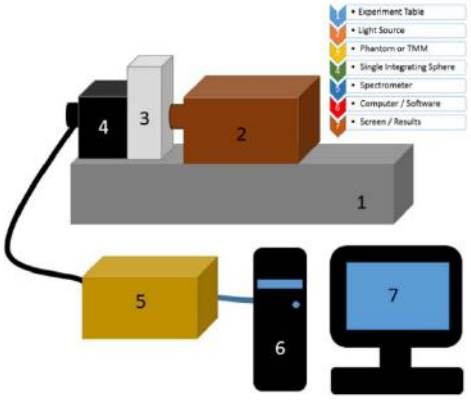

b)

Fig. 1. a) A picture showing the phantom measurement; b) Experiment set-up. 1-experimental table, 2-light source, 3-sample (phantom or TMM), 4-single integrating sphere, 5-compact spectrometer, 6-computer and 7-computer monitor.

ASSESSMENT OF THE OPTICAL DATA

First, the spectrum of the incoming light was obtained during the measurement. The light spectrum was received in the absence of the phantom material in the experimental setup for this. To remove the background noise in the dark environment, the same procedure was applied. The primary signal was then taken by subtracting the dark from the light. The phantom was then placed to the system, and the phantom's spectrum was recorded. The dark, which is background noise, was then eliminated to produce the real phantom signal. The I_o data is represented by the main signal, while the I signal is represented by the real phantom signal. Consequently, the following given formulas were used to extract macroscopic and microscopic optical characteristics from the acquired Main Signal (Light-Dark) and Real Phantom (Phantom-Dark) data.

CALCULATION OF OPTICAL PROPERTIES

Macroscopic optical properties such as absorbance, transmittance, reflectance, the refractive index, and

linear attenuation coefficient were measured and calculated by using the following formulas.

$$R+T+A = 1 \text{ or } \%R+\%T+\%A = \%100 \quad [45]\ (1)$$

Absorbance,

$$A;\ A=-\log(I/I_0)=-\log(T)=2-\log(\%T) \quad [46]\ (2)$$

$$\text{Transmittance, } T;\ T = I/I_0 \quad [46]\ (3)$$

$$\text{Reflectance, } R;\ R=1-(A+T) \quad [45]\ (4)$$

$$\text{Reflectance, } R = \frac{(n-1)^2}{(n+1)^2}, \quad [45]\ (5)$$

where n is the Refractive Index.

$$I = I_0 e^{-\mu x},\ \mu = -\frac{\ln \frac{I}{I_0}}{x} \quad [47]\ (6)$$

Where μ is the Linear Attenuation Coefficient.

The related microscopic optical formulas used in the calculations for absorption coefficient, scattering coefficient, reduced scattering coefficient, total attenuation coefficient and effective penetration depth are as in the following.

The Kubelka-Munk Function is given by;

$$F(R) = \frac{(1-R)^2}{2R} = \frac{k}{s} \quad [48]\ (7)$$

where R = Reflectance, k= Absorption Coefficient, s=Scattering Coefficient.

The total attenuation coefficient is described by;

$$\mu = \mu_t = \mu_a + \mu_s \quad [49]\ (8)$$

Where μ_a is Absorption Coefficient and μ_s is Scattering Coefficient.

That is, k=μ_a and s=μ_s can be matched by using (7) and (8) formulas.

The reduced scattering coefficient (μ_s') is defined by the following equation.

$$\mu_s' = (1-g)\mu_s \quad [50]\ (9)$$

Where g is the anisotropy factor. The g value of the phantom was used as 0.98 for the muscle phantom.

RESULTS AND DISCUSSION

Measurement results of macroscopic and microscopic optical parameters found in the study have been given below.

MEASUREMENT RESULTS OF MACROSCOPIC OPTICAL PARAMETERS

The typical determined macroscopic optical characteristics of the muscle phantom such as absorbance, transmittance, reflectance, refractive index, and optical linear attenuation coefficient can be seen from Figure 2 to Figure 6.

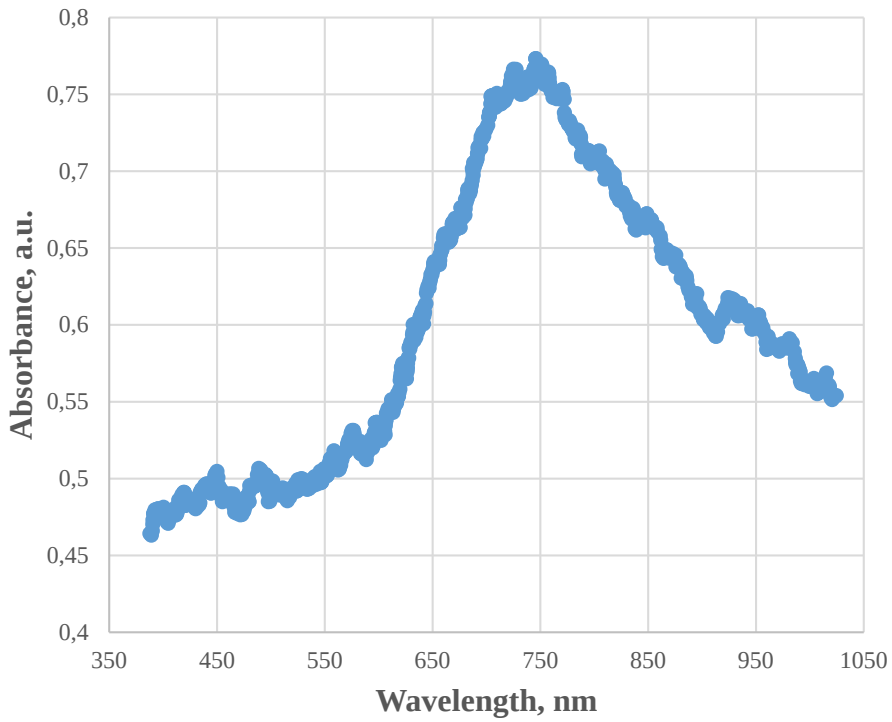

Fig. 2. Absorbance Spectrum of Muscle Phantom.

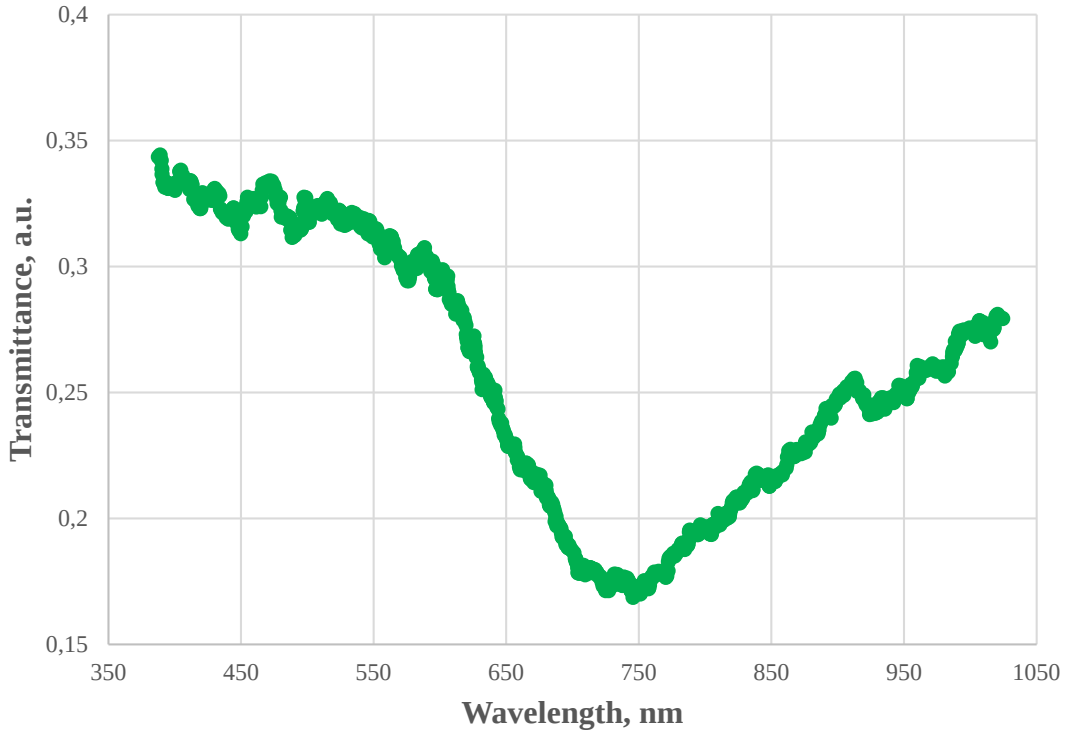

Fig. 3. Transmittance Spectrum of Muscle Phantom.

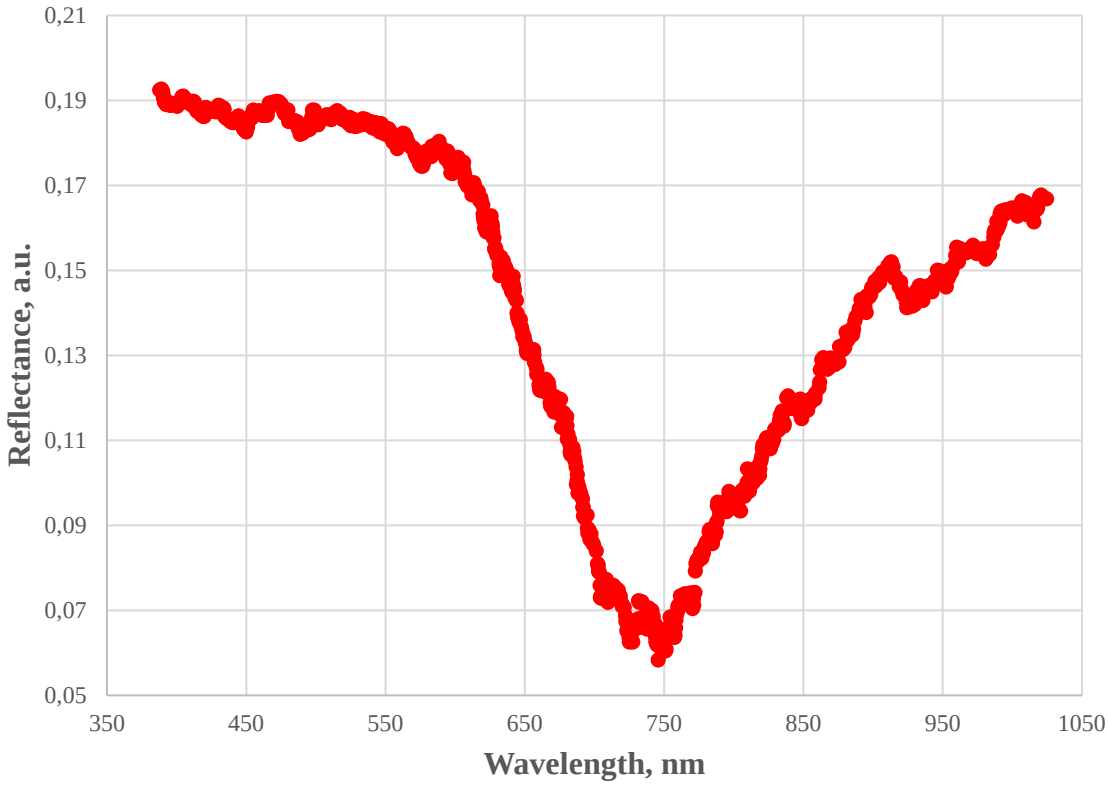

Fig. 4. Reflectance Spectrum of Muscle Phantom.

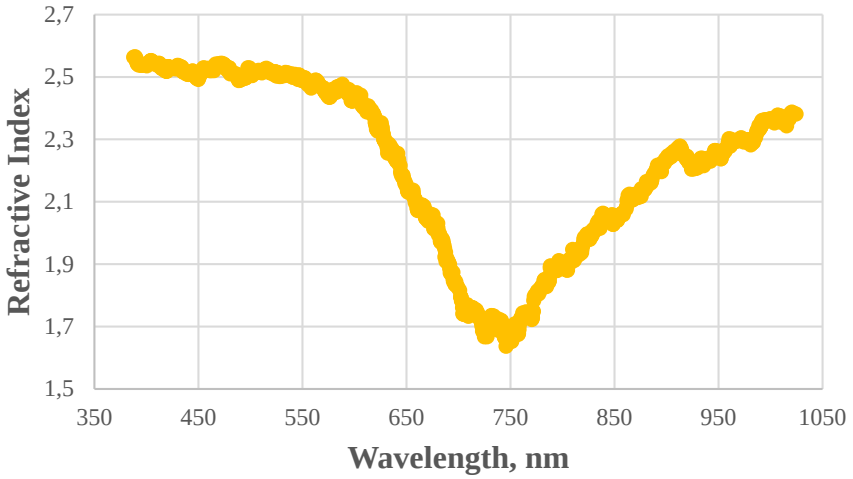

Fig. 5. Refractive Index Spectrum of Muscle Phantom.

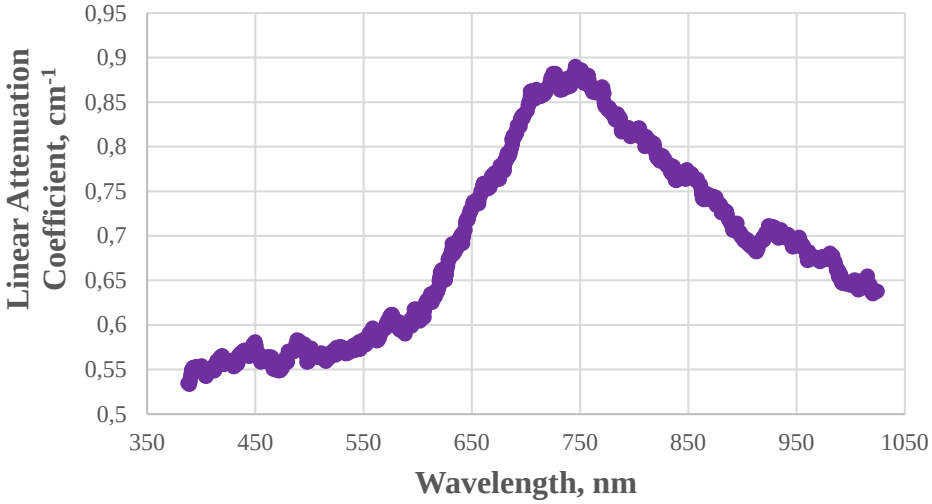

Fig. 6. Linear Attenuation Coefficient Spectrum of Muscle Phantom.

MEASUREMENT RESULTS OF MICROSCOPIC OPTICAL PARAMETERS

Figures 7 to 10 show the muscle phantom' typical determined microscopic optical characteristics such as absorption coefficient, scattering coefficient, and decreased scattering coefficient.

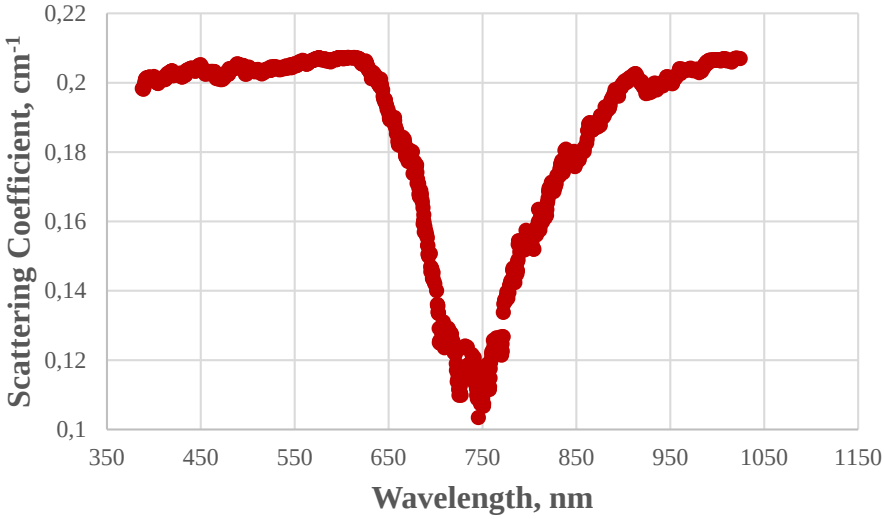

Fig. 7. Scattering Coefficient Spectrum of Muscle Phantom.

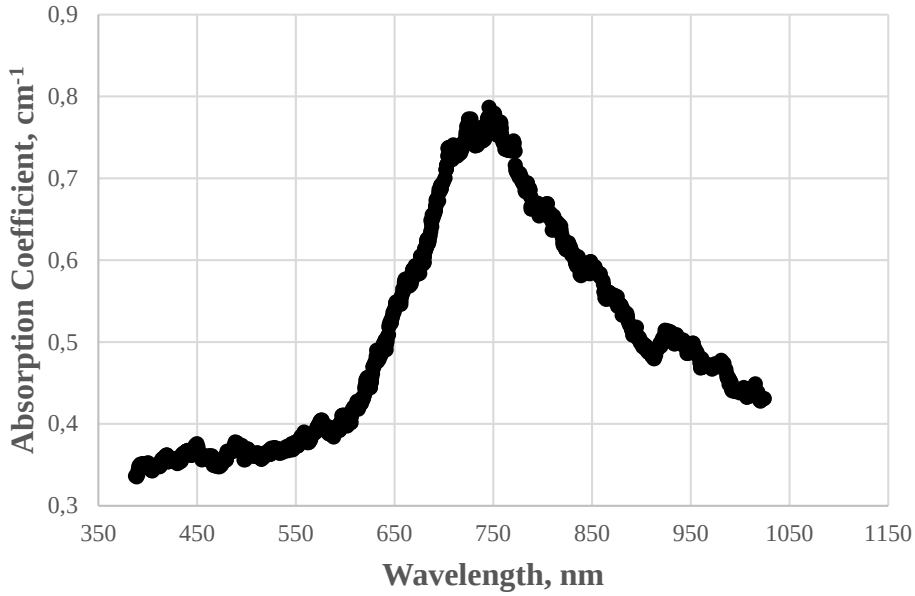

Fig. 8. Absorption Coefficient Spectrum of Muscle Phantom.

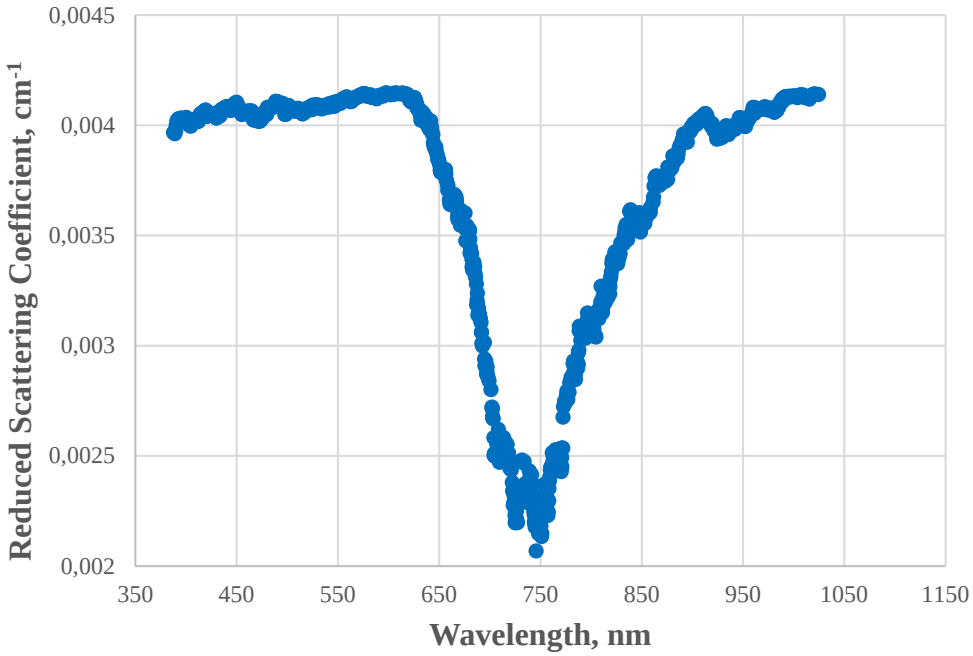

Fig. 9. Reduced Scattering Coefficient Spectrum of Muscle Phantom.

OPTICAL AND ACOUSTICAL PROPERTIES MEASUREMENTS

At least 6 measurements were taken while determining the optical properties of the muscle phantom. Typically, only one measurement is shown in the graphs shown above. Therefore, when we evaluate all the measurements together, the macroscopic optical properties of muscle phantom such as absorbance, transmittance, reflectance, refractive index and attenuation coefficient were calculated as average in the Table I.

Table I.

The measured macroscopic optical properties of the muscle phantom as average

Phantom	Transmittance T	Absorbance A	Reflectance R	Refractive Index
Muscle	0.71 ± 0.08	0.20 ± 0.03	0.09 ± 0.04	1.87 ± 0.28

By using these macroscopic optical properties, microscopic optical properties such as absorption coefficient, scattering coefficient, reduced scattering coefficient and total attenuation coefficient were calculated via Kubelka-Munk Function approach. We calculated μ_t from formula (6) and we know R = reflectance value, then we can solve these two equation [(7) and (8)] and find μ_a *and* μ_s. By the way, while calculating reduced scattering coefficient, we used 0.98 value for the muscle phantom. So, when we evaluate all the measurements together, the microscopic optical properties of muscle phantom such as absorption coefficient, scattering coefficient, the reduced scattering coefficient, and total attenuation coefficient were calculated as average in the Table II.

Table II.

The calculated microscopic optical properties of muscle phantom at around maximum absorbance peak.

Phantom	Absorption Coefficient, μ_a, cm^{-1}	Scattering Coefficient, μ_s, cm^{-1}	Reduced Scattering Coefficient, μ_s', cm^{-1}	Total Attenuation Coefficient, μ_t, cm^{-1}
Muscle	0.67 ± 0.14	0.14 ± 0.05	0.003 ± 0.001	0.82 ± 0.09

The produced muscle phantom was also ultrasonically tested by the pulse-echo method and the sound velocity was measured as 1550.9 ± 48.4 m/s.

DISCUSSION

In this study, macroscopic and microscopic optical properties of muscle phantom were investigated using a spectrometer with a single integrated sphere and a broadband white light source in the wavelength range of 200 nm to 1000 nm. In fact, spectra were originally taken between 200 nm and 1000 nm. However, since the resolution of the signals was very high, the noise level was also very high. Moving average of the data was taken to reduce the noise level and get more smoother signals. For this reason, the spectrum range in the graphics was obtained between 400 nm and 1000 nm. All the experiments done for optical measurements were carried out under controlled laboratory ambient conditions (Temperature was 23.5 °C ± 0.2 °C, and relative humidity was 50 rh% ± 2 rh%).

The fact that the phantom has the characteristics of a muscle phantom has been also verified with the literature by making both acoustical and optical measurements. The produced phantom was ultrasonically tested by the pulse-echo method in our laboratory and the sound velocity of 1547 m/s [51] declared in the literature for the muscle phantom was measured as 1550.9 m/s ± 48.4 m/s. Again, for optical characterization, the absorption coefficient can be taken as a reference. The absorbance peak values we found for the muscle phantom were in the range of 733.10 nm ± 57.33 nm and the absorption coefficient was found to be 0.067 mm^{-1} ± 0.014 mm^{-1}. The determined absorption coefficient value is in good agreement with the values given in the literature. For example, the absorption coefficients found for muscle tissue (e.g., porcine muscle and bovine muscle) performed as an in vitro study on animal tissues range from 0.053 mm^{-1} to 0.065 mm^{-1}[52].

As can be seen from the measurement results, the phantom sample is mostly opaque in the wavelength range of visible region and more absorption was observed at only around 733 nm. This shows that the material pigment forming the phantom has selective absorption at that wavelength. In addition, the opto-acoustical characterization results of the examined phantom were also found to be quite compatible with the values given in the literature.

CONCLUSION

In this study, the macroscopic and microscopic optical properties of the muscle phantom were determined using the method of Kubelka-Munk Function approach. In conclusion, optical characterization of phantoms can be easily done with this method and this method can also be applied to many kinds of phantom.

[1] *A.N. Bashkatov, K.V. Berezin, K.N. Dvoretskiy, M. L. Chernavina, E. A. Genina, V. D. Genin, V. V. Tuchin.* 2018. Measurement of tissue optical properties in the context of tissue optical clearing. Journal of biomedical optics, 23(9), 091416.

[2] *A.N. Bashkatov, E.A. Genina, V.V. Tuchin.* 2011. Optical properties of skin, subcutaneous, and muscle tissues: a review. Journal of Innovative Optical Health Sciences, 4(01), 9-38.

[3] *V.K. Nagarajan, J.M. Ward, B. Yu.* 2020. Association of liver tissue optical properties and thermal damage. Lasers in surgery and medicine, 52(8), 779-787.

[4] *Khaled T. Ramadan, Christopher McFadden, Bruno Gomes, Fynn Schwiegelshohn, Rafaela V.P. Ribeiro, Harley H.L. Chan, Vaughn Betz, Marcelo Cypel, Lothar Lilge.* Determination of Optical Properties and Photodynamic Threshold of Lung Tissue for Treatment Planning of In Vivo Lung Perfusion Assisted Photodynamic Therapy, Photodiagnosis and Photodynamic Therapy, Volume 35, 2021.

[5] *R. Rowland, A. Ponticorvo, A.J. Lopez, S. Li,*

X. Li, H. Ichii, A.J. Durkin. 2019. Monitoring kidney optical properties during cold storage preservation with spatial frequency domain imaging. Journal of biomedical optics, 24(11), 116003.

[6] *A.J. Costantino, C.J. Hyatt, M.C. Kollisch-Singule, J. Beaumont, B.J. Roth, A.M. Pertsov.* 2017. Determining the light scattering and absorption parameters from forward-directed flux measurements in cardiac tissue. Journal of biomedical optics, 22(7), 076009.

[7] *F. Bevilacqua, D. Piguet, P. Marquet, J.D. Gross, B.J. Tromberg, C. Depeursinge.* 1999. In vivo local determination of tissue optical properties: applications to human brain. Applied optics, 38(22), 4939-4950.

[8] *L. Spinelli, A. Torricelli, A.Pifferi, P. Taroni, G.M. Danesini, R. Cubeddu.* 2004. Bulk optical properties and tissue components in the female breast from multiwavelength time-resolved optical mammography. Journal of biomedical optics, 9(6), 1137-1142.

[9] *M.J. van Gemert, R. Verdaasdonk, E.G. Stassen, G.A. Schets, G.H. Gijsbers, J.J. Bonnier.* 1985. Optical properties of human blood vessel wall and plaque. Lasers in surgery and medicine, 5(3), 235-237.

[10] *T. Svensson, E. Alerstam, M. Einarsdóttír, K. Svanberg, S. Andersson-Engels.* 2008. Towards accurate in vivo spectroscopy of the human prostate. Journal of biophotonics, 1(3), 200-203.

[11] *H.J. Wei, G.Y.W. Da Xing, Y. Jin, H.M. Gu.* 2003. Optical properties of human normal small intestine tissue determined by Kubelka-Munk method in vitro. World journal of gastroenterology, 9(9), 2068.

[12] *T.J. Beck, W. Beyer, T. Pongratz, W. Stummer, R. Waidelich, H. Stepp, R. Baumgartner.* 2003, June. Clinical determination of tissue optical properties in vivo by spatially resolved reflectance measurements. In European conference on biomedical optics (p. 5138_96). Optical Society of America.

[13] *A. Pifferi, A.Torricelli, P. Taroni, A.L. Bassi, E. Chikoidze, E. Giambattistelli, R. Cubeddu.* 2004. Optical biopsy of bone tissue: a step toward the diagnosis of bone pathologies. Journal of biomedical optics, 9(3), 474-480.

[14] *S. Fantini, S.A. Walker, M.A. Franceschini, M. Kaschke, P.M. Schlag, K.T. Moesta.* 1998. Assessment of the size, position, and optical properties of breast tumors in vivo by noninvasive optical methods. Applied optics, 37(10), 1982-1989.

[15] *F. Fanjul-Vélez, J. L. Arce-Diego.* 2011, April. Light propagation in turbid media: Application to biological tissues. In Proceedings of 21st International Conference Radioelektronika 2011 (pp. 1-4). IEEE.

[16] *M.R. Shenoy, B.P. Pal.* 2008. Method to determine the optical properties of turbid media. Applied optics, 47(17), 3216-3220.

[17] *X. Liu, Y. Wu.* 2021. Monte-Carlo optical model coupled with Inverse Adding-Doubling for Building Integrated Photovoltaic smart window design and characterisation. Solar Energy Materials and Solar Cells, 223, 110972.

[18] *D. Sardar, L. Levy.* Optical Properties of Whole Blood. Lasers Med Sci 13, 106–111 (1998).

[19] *D.K. Sardar, B.G. Yust, F.J. Barrera, L.C. Mimun, A.T. Tsin.* 2009. Optical absorption and scattering of bovine cornea, lens and retina in the visible region. Lasers in medical science, 24(6), 839-847.

[20] *A. Shahin, W. Bachir, M.S. El-Daher.* 2021. Optical investigation of bovine grey and white matters in visible and near-infrared ranges. Polish Journal of Medical Physics and Engineering, 27(1), 99-107.

[21] *M.M. Pérez, A. Ionescu, A. Yebra, J.C. Cardona, L.J. Herrera, M.J. Rivas, R. Ghinea.* 2017, August. Researching in biomaterials optics. In Third International Conference on Applications of Optics and Photonics (Vol. 10453, p. 104532M). International Society for Optics and Photonics.

[22] *E. Zamora-Rojas, B. Aernouts, A. Garrido-Varo, W. Saeys, D. Pérez-Marín, J.E. Guerrero-Ginel.* 2013. Optical properties of pig skin epidermis and dermis estimated with double integrating spheres measurements. Innovative Food Science & Emerging Technologies, 20, 343-349.

[23] *B. Karaböce.* 2015, May. Focused ultrasound temperature effect in tissue-mimicking material and sheep liver. In 2015 IEEE International Symposium on Medical Measurements and Applications (MeMeA) Proceedings (pp. 131-134). IEEE.

[24] *B. Karaböce, H.O. Durmuş.* 2015. Visual investigation of heating effect in liver and lung induced by a HIFU transducer. Physics Procedia, 70, 1225-1228.

[25] *B. Karaböce, E. Çetin, H.O. Durmuş.* 2016, May. Investigation of temperature rise in tissue—Mimicking material induced by a HIFU transducer. In 2016 IEEE International Symposium on Medical Measurements and Applications (MeMeA) (pp. 1-6). IEEE.

[26] *B. Karaböce, E. Çetin, H.O. Durmuş, M. Özdingiş, H. Öztürk, K. Mahmat, M.A. Güler.* 2018, June. Investigation of Different TMMs in High Intensity Focused Ultrasound Applications. In 2018 IEEE International Symposium on Medical Measurements and Applications (MeMeA) (pp. 1-5). IEEE.

[27] *B.W. Pogue, M.S. Patterson.* 2006. Review of tissue simulating phantoms for optical spectroscopy, imaging and dosimetry. Journal of biomedical optics, 11(4), 041102.

[28] *İ. Akkaya, M. Engin, Y. Öztürk.* Doku Fantom Üretimi ve Temel Optik Özelliklerinin Ölçümü/Fabrication of Tissue Phantom and Measurement of The Fundamental Optical Properties. Celal Bayar Üniversitesi Fen Bilimleri Dergisi, 13(1), 2017, 205-209.

[29] *J. Zhang, L.I.U.Yuanjie, J. Robic, A. Nkengne, Y.A.N. Hong, X. Zhang, X.Y. Soo.* 2019. Optical Phantom Development for Skin Measurement. In 19th International Congress of Metrology (CIM2019) (p. 19001). EDP Sciences.

[30] *R. Srinivasan, D. Kumar, M. Singh.* 2002. Optical tissue-equivalent phantoms for medical imaging. Trends Biomater. Artif. Organs, 15(2), 42-47.

[31] *R.A. Jaime, R.L. Basto, B. Lamien, H.R. Orlande, S. Eibner, O. Fudym.* 2013. Fabrication methods of phantoms simulating optical and thermal properties. Procedia Engineering, 59, 30-36.

[32] *A.I. Chen, M.L.Balter, M.I.Chen, D. Gross, S.K. Alam, T.J. Maguire, M.L. Yarmush.* 2016. Multilayered tissue mimicking skin and vessel phantoms with tunable mechanical, optical, and acoustic properties. Medical Physics, 43 (6), 3117-3131.

[33] *P. Lai, X. Xu, L.V. Wang.* 2014. Dependence of optical scattering from Intralipid in gelatin-gel based tissue-mimicking phantoms on mixing temperature and time. Journal of biomedical optics, 19(3), 035002.

[34] *E. Dong, Z. Zhao, M. Wang, Y. Xie, S. Li, P. Shao, R.X. Xu.* 2015. Three-dimensional fuse deposition modeling of tissue-simulating phantom for biomedical optical imaging. Journal of biomedical optics, 20(12), 121311.

[35] https://www.medicalnewstoday.com/articles/321617#eleven-main-functions-of-the-muscular-system

[36] https://www.medicalnewstoday.com/articles/249192#summary

[37] *McGraw-Hill.* Dictionary of Scientific & Technical Terms, 6E, Copyright © 2003 by The McGraw-Hill Companies, Inc.

[38] *L.Yang, B. Kruse.* 2004. Revised Kubelka–Munk theory. I. Theory and application. JOSA A, 21(10), 1933-1941.

[39] *W.E. Vargas, G.A. Niklasson.* 1997. Applicability conditions of the Kubelka–Munk theory. Applied optics, 36(22), 5580-5586.

[40] *A.B. Murphy.* 2006. Modified Kubelka–Munk model for calculation of the reflectance of coatings with optically-rough surfaces. Journal of Physics D: Applied Physics, 39(16), 3571.

[41] *T. Lindbergh, M. Larsson, I. Fredriksson, T. Strömberg.* 2007, February. Reduced scattering coefficient determination by non-contact oblique angle illumination: methodological considerations. In Optical Interactions with Tissue and Cells XVIII (Vol. 6435, p. 64350I). International Society for Optics and Photonics.

[42] *C.J. Hourdakis, A. Perris.* 1995. A Monte Carlo estimation of tissue optical properties for use in laser dosimetry. Physics in Medicine & Biology, 40(3), 351.

[43] *M.I. Gutierrez, S.A. Lopez-Haro, A. Vera, L. Leija.* 2016. Experimental verification of modeled thermal distribution produced by a piston source in physiotherapy ultrasound. BioMed research international, 2016.

[44] *T.D. Mast.* 2000. Empirical relationships between acoustic parameters in human soft tissues. Acoustics Research Letters Online, 1(2), 37-42.

[45] *M.Y. Nadeem, W. Ahmed.* 2000. Optical properties of ZnS thin films. Turkish Journal of Physics, 24(5), 651-659.

[46] *D.T. Harvey.* 2003. Analytical Chemistry for Technicians, 3rd Edittion, page 193, (John Kenkel).

[47] *S. Chang, A.K. Bowden.* 2019. Review of methods and applications of attenuation coefficient measurements with optical coherence tomography. Journal of biomedical optics, 24(9), 090901.

[48] *J.O.S.E. Torrent, V. Barrón.* 2008. Diffuse reflectance spectroscopy. Methods of Soil Analysis Part 5—Mineralogical Methods, 5, 367-385.

[49] *B.C. Wilson.* 1995. Measurement of tissue optical properties: methods and theories. In Optical-thermal response of laser-irradiated tissue (pp. 233-303). Springer, Boston, MA.

[50] *E.J. Jeong, H.W. Song, Y.J. Lee, S.J. Park, M.J. Yim, S.S. Lee, B.K. Kim.* (2017). Fabrication and characterization of PVCP human breast tissue-mimicking phantom for photoacoustic imaging. BioChip Journal, 11(1), 67-75.

[51] *T.D. Mast.* 2000. Empirical relationships between acoustic parameters in human soft tissues. Acoustics Research Letters Online, 1(2), 37-42.

[52] *P. Sun, Y. Wang.* 2010. Measurements of optical parameters of phantom solution and bulk animal tissues in vitro at 650 nm. Optics & Laser Technology, 42(1), 1-7.